

# Tumor-Derived EV-Encapsulated miR-181b-5p Induces Angiogenesis to Foster Tumorigenesis and Metastasis of ESCC

Ying Wang,<sup>1,2,3</sup> Jiqiang Lu,<sup>1,2,3</sup> Lin Chen,<sup>1,2</sup> Huan Bian,<sup>1,2</sup> Jialiang Hu,<sup>1,2</sup> Dongping Li,<sup>1,2</sup> Chunlei Xia,<sup>1,2</sup> and Hanmei Xu<sup>1,2</sup>

<sup>1</sup>The Engineering Research Center of Synthetic Peptide Drug Discovery and Evaluation of Jiangsu Province, China Pharmaceutical University, Nanjing 210009, China;

<sup>2</sup>State Key Laboratory of Natural Medicines, Ministry of Education, China Pharmaceutical University, Nanjing 210009, China

**Pathological angiogenesis is necessary for tumor development and metastasis. Tumor-derived extracellular vesicles (EVs) play an important role in mediating the crosstalk between cancer cells and vascular endothelial cells. To date, whether and how microRNAs (miRNAs) encapsulated in tumor-derived EVs affect angiogenesis in esophageal squamous cell carcinoma (ESCC) remains unclear. Here, we showed that miR-181b-5p, an angiogenesis-promoting miRNA of ESCC, can be transferred from ESCC cells to vascular endothelial cells via EVs. In addition, ESCC-derived EVs-miR-181b-5p dramatically induced angiogenesis by targeting PTEN and PHLPP2, and thereby facilitated tumor growth and metastasis. Moreover, miR-181b-5p was highly expressed in ESCC tissues and serum EVs. High miR-181b-5p expression level in ESCC patients was well predicted for poor overall survival. Our work suggests that intercellular crosstalk between tumor cells and vascular endothelial cells is mediated by tumor-derived EVs. miR-181b-5p-enriched EVs secreted from ESCC cells are involved in angiogenesis that control metastasis of ESCC, providing a potential diagnostic biomarker or drug target for ESCC patients.**

## INTRODUCTION

Esophageal cancer (EC) stands as the eighth most commonly diagnosed cancer in the world and is the sixth leading cause of cancer-related mortality.<sup>1,2</sup> It has two dominant histological types: esophageal adenocarcinoma (ECA) and esophageal squamous cell carcinoma (ESCC).<sup>3,4</sup> ESCC is especially frequent in males (>4:1) and has an especially high incidence in Asia. ESCC has a particularly poor prognosis with 5-year survival rates rarely exceeding 20%,<sup>5</sup> suggesting that primary and secondary prevention is key to reducing mortality from this disease. Early detection of ESCC is critical because disease prognosis and management are determined by the stage at which ESCC is diagnosed.<sup>2</sup> Molecular profiling of ESCC tumors has shown promise in identifying markers for early detection and treatment. Thus, revealing the molecular mechanism of ESCC tumorigenesis and metastasis may help provide novel biomarkers and potential drug targets for clinical diagnosis and prognosis of ESCC patients. Angiogenesis refers to the growth of new blood vessels from preexisting capillaries,<sup>6</sup> which plays a pivotal role in tumor growth, progression, invasiveness, and

metastasis.<sup>7</sup> Neovascularization supplies oxygen and nutrients to proliferative tumor cells and serves as a conduit for tumor cells metastasis.<sup>8</sup> Therefore, targeting and regulating the angiogenesis process is an effective anti-cancer therapeutic strategy.<sup>9</sup>

Extracellular vesicles (EVs) are membranous vesicles of approximately 30–300 nm in diameter containing cytosols and functional biomolecules from parental cells, including microRNAs (miRNAs), long non-coding RNAs (lncRNAs), messenger RNAs (mRNA), transcription factors, cytokines, and growth factors.<sup>10</sup> EVs can be produced by various types of cells and serve as mediators in intercellular communications by transporting information cargo.<sup>11</sup> Increasing evidence has implicated that tumor-released EVs induce alterations in their recipient cells, thereby playing a role in tumor growth, metastasis, and angiogenesis.<sup>12,13</sup> Moreover, recent studies have demonstrated that EVs are potentially useful for cancer diagnosis as biomarkers in circulating serum.<sup>14</sup> In view of the biological function of EVs, we speculated that EVs carrying tumor-derived miRNAs can transfer into vascular endothelial cells and activate angiogenesis-related signaling pathways.

miRNAs are a class of short endogenous non-coding RNAs of 21–23 nt that promote the cleavage of the target mRNAs or inhibit its translation through complementary base pairing at the 3' untranslated region (UTR).<sup>15,16</sup> They negatively regulate the expression of target genes at a posttranscriptional level, thereby affecting various cellular processes, such as cell proliferation, differentiation, aging, and apoptosis.<sup>17,18</sup> An increasing number of miRNAs have been identified to be involved in angiogenic signaling pathways by regulating angiogenic growth factors, promoting tumor cell migration, and fostering the epithelial-mesenchymal transition (EMT) process.<sup>19–25</sup>

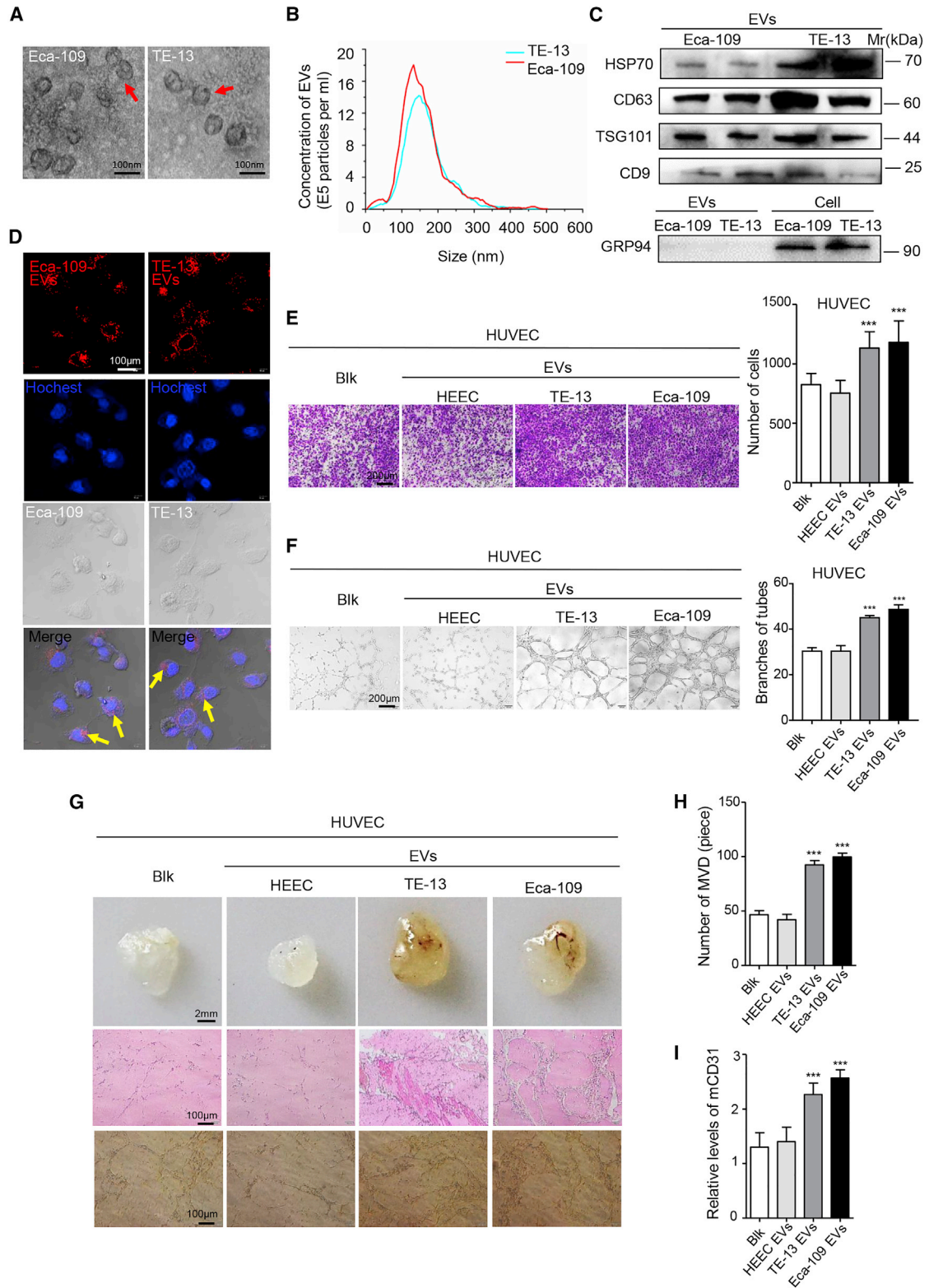
Received 11 February 2020; accepted 10 March 2020;  
<https://doi.org/10.1016/j.omtn.2020.03.002>.

<sup>3</sup>These authors contributed equally to this work.

**Correspondence:** Hanmei Xu, The Engineering Research Center of Synthetic Peptide Drug Discovery and Evaluation of Jiangsu Province, China Pharmaceutical University, Nanjing 210009, China.

**E-mail:** [13913925346@126.com](mailto:13913925346@126.com)





(legend on next page)

Although previous studies have reported that miRNAs play an important role in the establishment of pro-angiogenic tumor microenvironment,<sup>12,26,27</sup> the mechanism of miRNAs in tumor-derived EVs regulating angiogenesis in ESCC is still unclear.

In this study, we identified that miR-181b-5p was highly expressed in ESCC tissues and EVs. The biological function of vascular endothelial cells was significantly enhanced by co-incubation with EVs isolated from ESCC cells. We found that ESCC-derived EVs-miR-181b-5p can be transferred to vascular endothelial cells and targeted phosphatase and tensin homolog (PTEN) and PH domain and Leucine rich repeat Protein Phosphatases 2 (PHLPP2), thereby activating Akt signaling to promote angiogenesis. In addition, we demonstrated that EVs-miR-181b-5p promoted the ESCC tumor growth and consequently metastasis in nude mice by inducing angiogenesis. Finally, our clinical data suggested that high miR-181b-5p expression level in ESCC patients was correlated with poor prognosis. These findings suggest that miRNAs in tumor-derived EVs play an important role in intercellular communication during angiogenesis and implicate that antagonism of EVs-miR-181b-5p represents a potential therapeutic strategy for cancer therapy.

## RESULTS

### Tumor-Derived EVs Regulate Angiogenesis in ESCC

In light of the fact that EV secretion is an important way for tumors to induce systemic changes, it rationally leads to the question whether EVs participate in angiogenesis during ESCC development. We first determined whether cancer cells can secrete EVs that are then transported into target cells. To make it clear, two ESCC cell lines were chosen, Eca-109 and TE-13. First, we isolated and purified the particles from conditioned media of tumor cells. Electron microscopy (Figure 1A) and NanoSight analysis (Figure 1B) revealed that particles isolated by ultracentrifugation contained abundant ESCC-derived EVs with a diameter of 30–300 nm (Figure 1B). Western blot analysis confirmed that these particles expressed EV-specific protein markers HSP70, CD63, TSG101, and CD9, whereas the endoplasmic reticulum protein Grp94 was present only in ESCC cells, but not in ESCC-derived EVs (Figure 1C). Human umbilical vein endothelial cells (HUVECs), derived from the endothelium of veins from the umbilical cord, were chosen as a model system for the study of the function and pathology of human vascular endothelial cell.<sup>28</sup> Next, we tested whether these ESCC-derived EVs can be taken up by HUVECs. These ESCC-derived EVs were labeled with the fluorescent dye PKH26 and then added into

the culture medium of HUVECs. After 12 h, HUVECs exhibited efficient uptake of the ESCC-derived EVs, as indicated by the presence of red fluorescence staining in these cells (Figure 1D). Overall, our results show that ESCC cell lines can secrete EVs, which are then efficiently taken up by recipient cells.

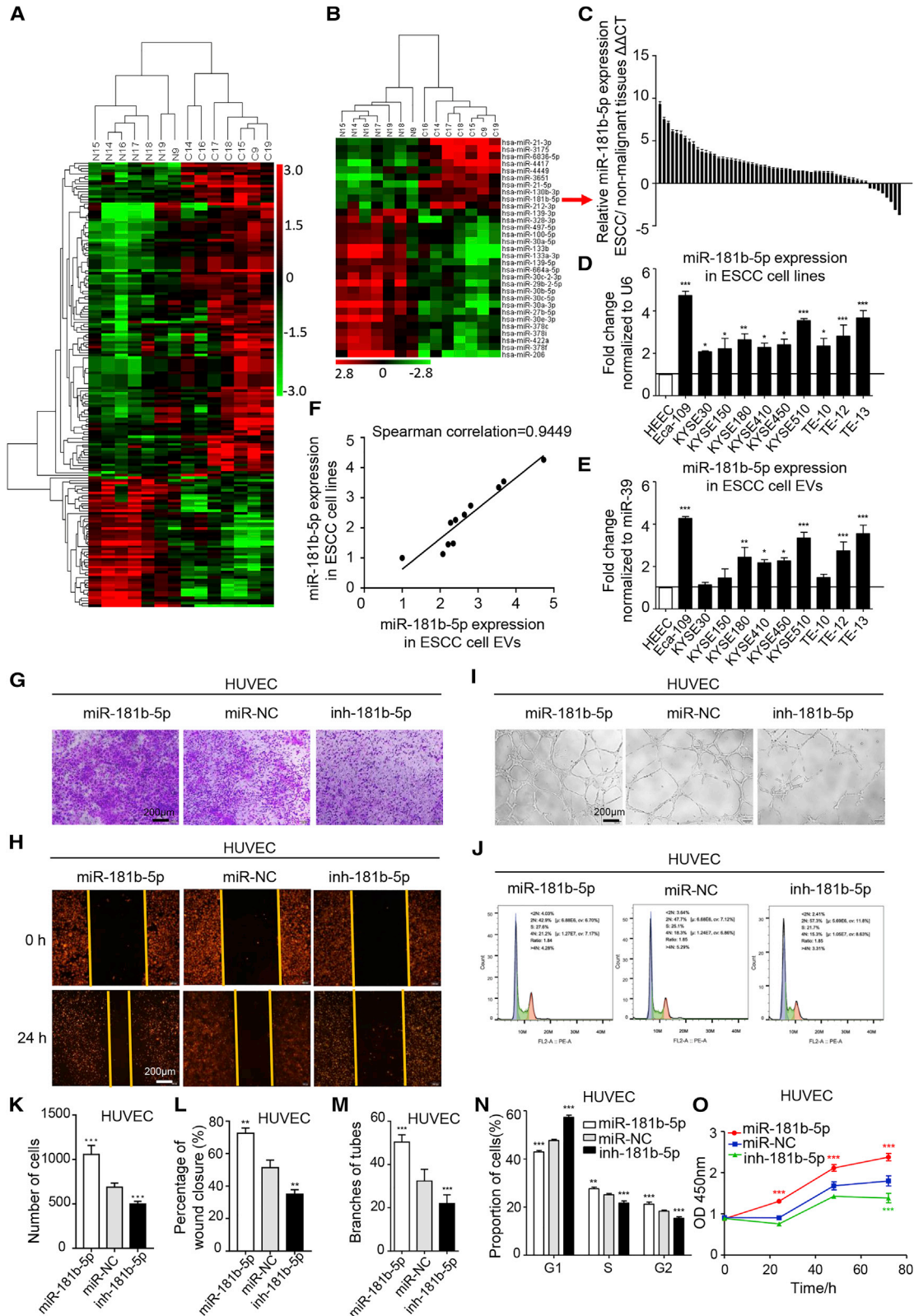
To explore the biological functions of ESCC-derived EVs on HUVECs, we co-incubated EVs derived from normal esophageal epithelial cells (HEECs) or ESCC cells with HUVECs *in vitro*. Migration assays showed that more HUVECs migrated after co-incubation with ESCC-derived EVs, compared with HEEC-derived EVs (Figure 1E). Wound healing assays further confirmed that ESCC-derived EVs could remarkably improve HUVEC migratory ability (Figures S1A and S1B). Cell viability and cell-cycle assays showed that ESCC-derived EVs could promote HUVEC proliferative capacity and cell-cycle progression (Figures S1C–S1E). We next examined that ESCC-derived EVs universally enhanced HUVEC tubulogenesis (Figure 1F). To further evaluate the mediation of EVs in angiogenesis, EVs within Matrigel were subcutaneously injected into nude mice, exhibiting a significant difference in vessel formation between ESCC-derived and HEEC-derived EVs. HUVECs cocultured with ESCC-derived EVs dramatically increased angiogenesis (Figures 1G–1I). Altogether, the above results suggest that EVs derived from ESCC contribute to tumor angiogenesis.

### EVs-miR-181b-5p Is Highly Expressed and Mediates Angiogenesis in ESCC

We next explored how ESCC-derived EVs accelerate tumor angiogenesis. Abundant miRNAs are encapsulated in EVs and have an important role in cell-cell communications.<sup>29</sup> Therefore, we hypothesized that miRNAs in tumor-derived EVs may mediate angiogenesis in ESCC. To identify the specific miRNAs involved, we conducted microarrays to generate miRNA profiles of ESCC tissues and adjacent normal tissues from seven ESCC patients (Table S1). Comparison of differently expressed miRNAs was calculated by single channel chip and normalized by Lowess, and the results were compared and shown as heatmaps in Figure 2A. Ten of the most upregulated miRNAs (fold change  $\geq 2.5$ ;  $p \leq 0.001$ ) in ESCC tissues were subjected to validation (Figure 2B). miR-181b-5p was the most highly expressed in 58 pairs of ESCC tissues compared with adjacent nonmalignant tissues (Figures 2C and S2A). More importantly, miR-181b-5p expression was also validated to be elevated in 10 ESCC cell lines and ESCC cell EVs, compared with HEECs (Figures 2D and 2E),

#### Figure 1. EVs Secreted from ESCC Cells Contribute to Angiogenesis *In Vitro* and *In Vivo*

(A) EVs released by Eca-109 and TE-13 cells were observed by electron microscopy. Scale bars, 100 nm. (B) The concentration of EVs was detected by NanoSight particle tracking analysis. (C) Indicated proteins in EVs were detected by western blot. (D) The delivery of PKH26-labeled (red) EVs to Hoechst-labeled HUVECs (blue) was shown by confocal imaging. Yellow arrows represented delivered EVs, and representative images were presented. Scale bar, 100  $\mu\text{m}$ . (E) Migration assays of HUVECs treated with equal quantities of EVs derived from HEEC and ESCC cell lines or blank control. Migrated cells were counted, and representative images were shown. Scale bar, 200  $\mu\text{m}$ . (F) Tube formation assays of HUVECs treated with equal quantities of EVs derived from HEEC and ESCC cell lines or blank control. Branches of tubes were counted, and representative images were shown. Scale bar, 200  $\mu\text{m}$ . (G) Matrigel mixed with ESCC-derived EVs or PBS was subcutaneously injected into nude mice ( $n = 5$ ). After 14 days, the Matrigel plugs were harvested and performed by hematoxylin and eosin staining and immunohistochemistry for CD31. Representative micrographs were shown. Scale bars, 2 mm (top panels); 100  $\mu\text{m}$  (middle and bottom panels). (H) The number of microvessel density (MVD) significantly increased in the Matrigel plugs containing ESCC-derived EVs. (I) The expression of mouse CD31 was significantly increased in the Matrigel plugs containing ESCC-derived EVs. Experiments were performed at least in triplicate, and results are shown as mean  $\pm$  SD. Student's *t* test was used to analyze the data. \* $p < 0.05$ ; \*\* $p < 0.01$ ; \*\*\* $p < 0.001$ .



(legend on next page)

and exhibited a high correlation score (Figure 2F). In addition, targets of miR-181b-5p were directly involved in the phosphatidylinositol signaling pathway of Kyoto Encyclopedia of Genes and Genomes (KEGG) database (Figure S2B). Surprisingly, we found that the expression of EVs-miR-181b-5p was positively correlated with the metastasis in the different ESCC cell lines (Figures S2C–S2E). The 58 patients were divided into miR-181b-5p-high (n = 29, with an average  $\Delta\text{Ct} = 11.89$ ) and miR-181b-5p-low (n = 29, with an average  $\Delta\text{Ct} = 14.53$ ) groups using the median expression level of miR-181b-5p as a cutoff ( $\Delta\text{Ct} = 12.97$ ). We found that high miR-181b-5p expression was notably correlated with high advanced TNM stage (N stage,  $p = 0.008$ ; clinical stage,  $p = 0.003$ ; Table S2). These data indicated that overexpression of miR-181b-5p was strongly associated with poor clinicopathological characteristics of ESCC patients.

To further validate whether the role of miR-181b-5p was associated with angiogenesis, we transiently transfected HUVECs with miR-181b-5p mimic, inhibitor, and negative control, respectively (Figure S3A). *In vitro* assay illustrated that miR-181b-5p induced HUVEC migration and proliferation, and promoted cell-cycle progression and tube formation (Figures 2G–2O). Furthermore, we investigated the functional role of EVs-miR-181b-5p in mediating angiogenesis; Eca-109 cells were transfected with locked nucleic acid (LNA)-miR-181b-5p mimic and LNA-miR-181b-5p inhibitor and compared with an equivalent control vector to establish the Eca-109/miR-181b-5p cells, Eca-109/inh-181b-5p cells, and Eca-109/miR-NC cells (Figure S3B). EVs from Eca-109/miR-181b-5p cells enhanced cell growth and migration, and facilitated the progress of cell-cycle and tube formation of HUVECs, whereas inhibiting miR-181b-5p expression attenuated these functions (Figures S3C–S3G). Similar results were obtained when HUVECs were treated with conditioned medium (CM) from indicated tumor cells (Figures S4A–S4E). More importantly, as shown in Figures S5A and S5B, co-culture with Eca-109/miR-181b-5p cells significantly enhanced HUVEC proliferation and tubulogenesis, compared with co-culture with Eca-109/miR-NC cells. However, these phenotypes were blocked by prior addition of the EV secretion inhibitor GW4869 to Eca-109 cells, showing that ESCC cells regulate angiogenesis via EVs-miR-181b-5p.

### PTEN and PHLPP2 Are Direct Downstream Targets of miR-181b-5p in Mediating Angiogenesis

To identify the targets of EVs-miR-181b-5p in HUVECs, we used two bioinformatics tools (TargetScan and miRDB) to predict a set

of common target genes. Among them, PTEN and PHLPP2 were overlapped among all databases and verified to be responsible for angiogenesis (Figure 3A). First, we confirmed that PTEN and PHLPP2 expression could be downregulated in HUVECs by miR-181b-5p or Eca-109/miR-181b-5p EVs at protein levels. However, the levels of PTEN and PHLPP2 mRNA were essentially unchanged regardless of whether the cells were transfected with miR-181b-5p or treated with Eca-109/miR-181b-5p EVs (Figures 3B, S6A, and S6B). Then the alignment between miR-181b-5p sequence and the full length of PTEN or PHLPP2 sequence was determined to show that 3' UTRs of PTEN and PHLPP2 were potential targets of miR-181b-5p (Figure 3C). Subsequently, the wild-type and mutated miR-181b-5p binding site were cloned into the luciferase vectors. It was obvious that luciferase activity decreased markedly in HUVECs co-transfected with the wild-type binding site vector in the presence of miR-181b-5p. However, cells containing the mutated binding site vector did not show such repression (Figure 3D). Similarly, the luciferase activity was remarkably decreased only in HUVECs transfected with wild-type binding site vector of PTEN or PHLPP2 after treatment with Eca-109/miR-181b-5p EVs (Figures S6C and S6D). These results reveal that PTEN and PHLPP2 are direct targets of miR-181b-5p in HUVECs.

Furthermore, to confirm that PTEN and PHLPP2 acted as downstream target genes of miR-181b-5p in ESCC, we performed migration assays and tube formation assays. As shown in Figures 3E and 3F, miR-181b-5p exhibited a promotion on motility and tubulogenesis of HUVECs. However, overexpression of full-length PTEN or PHLPP2 (Figures S6E and S6F) could neutralize the effect of miR-181b-5p on angiogenesis. Moreover, small interfering RNAs (siRNAs) targeting PTEN or PHLPP2 (Figures S6G and S6H) eliminated the suppression of angiogenesis by miR-181b-5p inhibitors (Figures S7A and S7B). Overall, these results suggest that ESCC-derived EVs-miR-181b-5p induces angiogenesis by directly targeting PTEN and PHLPP2.

### EVs-miR-181b-5p Regulates Angiogenesis via the Akt Signaling Pathway

Results above showed that ESCC-derived EVs-miR-181b-5p enhanced motility and tubulogenesis of HUVECs by downregulating the expression of PTEN and PHLPP2, which function as tumor suppressors by negatively regulating the Akt signaling pathway. Next, we detected Akt signaling in our experiment models. As shown

### Figure 2. EVs-miR-181b-5p Is Highly Expressed in ESCC and Mediates Angiogenesis *In Vitro*

(A) Microarray analysis of significantly expressed miRNAs in ESCC tissues and adjacent normal tissue miRNA from seven ESCC patients was presented in a heatmap. (B) Hierarchical clustering analysis of 10 of the most upregulated and 21 of the most downregulated miRNAs (fold change  $> 2.5$  or  $< -2.5$ ;  $p < 0.001$ ) was shown. (C) The expression of miR-181b-5p in 58 pairs of ESCC tissues was detected by qRT-PCR.  $\Delta\Delta\text{Ct} = -((\text{Ct}_{\text{miR-181b-5p}} - \text{Ct}_{\text{U6}})_{\text{ESCC}} - (\text{Ct}_{\text{miR-181b-5p}} - \text{Ct}_{\text{U6}})_{\text{corresponding non-malignant tissue}})$ . (D) The expression of miR-181b-5p in 10 ESCC cell lines compared with normal esophageal epithelia cells (HEEC) was detected by quantitative relative real-time PCR. (E) The expression of miR-181b-5p in EVs from the cell lines referred above was detected by quantitative relative real-time PCR. (F) Significant correlation of miR-181b-5p expression in ESCC cells and ESCC cell-derived EVs was calculated with Spearman's test. (G–O) Migration (G and K), wound healing (H and L), tube formation (I and M), cell cycle (J and N), and cell viability (O) assays of HUVECs treated with miR-181b-5p mimic, inhibitor, or negative control *in vitro*. Representative images and quantitative analysis were shown. Scale bars, 200  $\mu\text{m}$ . Each experiment was performed three times independently, and data are shown as mean  $\pm$  SD. Student's *t* test was used to analyze the data (\* $p < 0.05$ ; \*\* $p < 0.01$ ; \*\*\* $p < 0.001$ ).

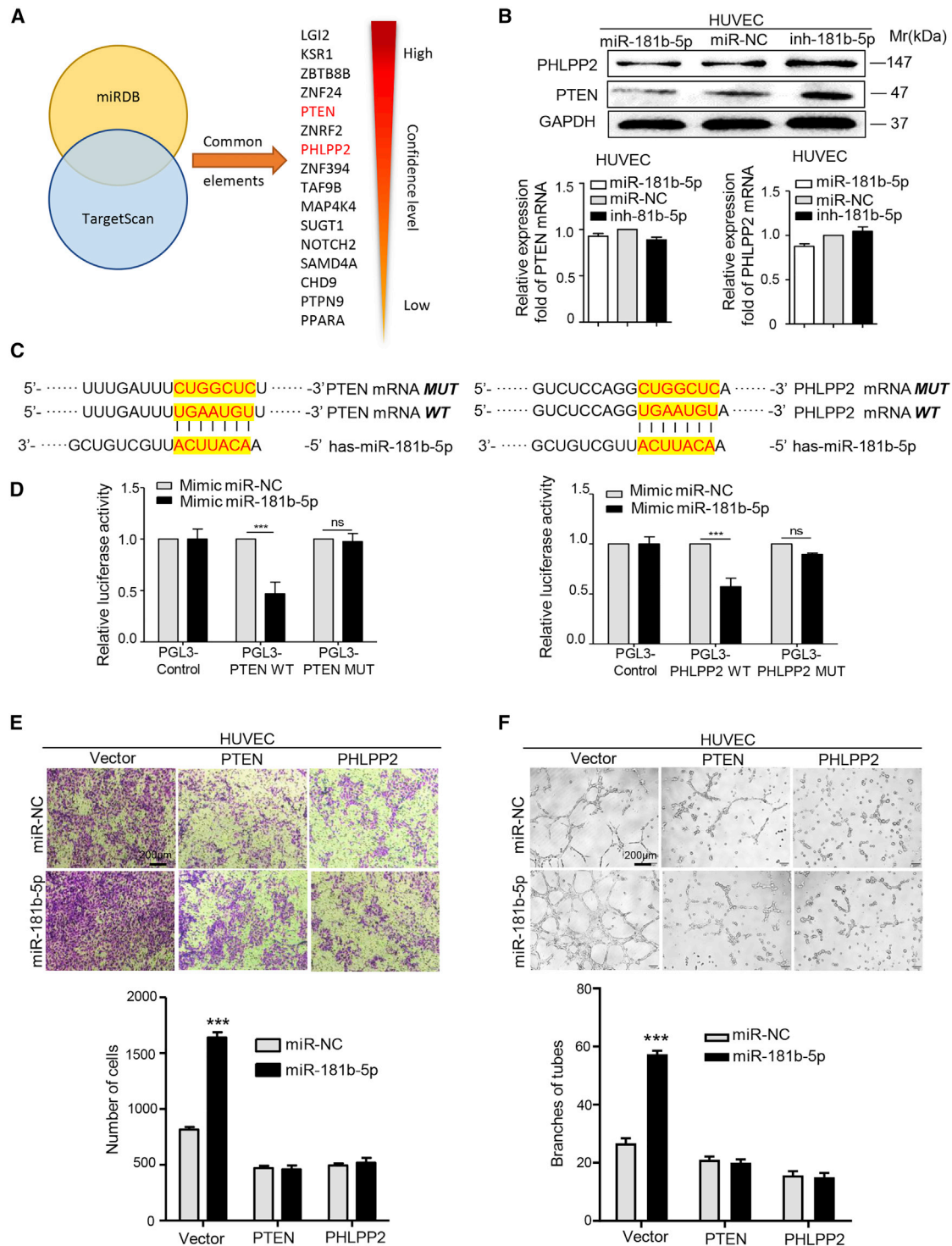


**Figure 3. PTEN and PHLPP2 Are Direct Downstream Targets of miR-181b-5p in Mediating Angiogenesis**

(A) Target gene prediction of miR-181b-5p with two bioinformatics tools, miRDB and TargetScan. (B) Quantitative relative real-time PCR and western blot assays of PTEN and PHLPP2 expression in HUVECs treated with miR-181b-5p mimic, inhibitor, or negative control. (C) The wild-type and a mutated type of binding site between miR-181b-5p

(legend continued on next page)

in Figure 4A, CM of ESCC cells promoted phosphorylated Akt (p-Akt) expression and activation of this signaling pathway in HUVECs, as compared with CM of HEEC cells. Similar results were obtained when HUVECs were treated with EVs from indicated tumor cells (Figure 4B). Furthermore, miR-181b-5p expression or PTEN/PHLPP2 suppression also promoted Akt phosphorylation (Figure 4C), whereas overexpression of PTEN/PHLPP2 suppressed Akt phosphorylation (Figure 4C). All of these data indicate that miR-181b-5p induces angiogenesis by mediating Akt signaling activation.

Vascular morphogenesis and homeostasis are complex biological processes that are tightly controlled by multiple signaling pathways. Among them, the role of Akt signaling in the mediation of angiopoietin 1 (Ang1), Ang2, and endothelial nitric oxide synthase (eNOS) induced by miR-181b-5p is worthy of investigating. Immunoblotting analyses showed that p-Akt, Ang1, and eNOS expression were promoted, whereas Ang2 expression was depressed by miR-181b-5p mimic or PTEN/PHLPP2 knockdown; however, it was reversed by overexpression of PTEN/PHLPP2 (Figure 4C). In addition, compared with Eca-109/miR-NC EVs, Eca-109/miR-181b-5p EVs dramatically decreased the expression levels of PTEN, PHLPP2, and Ang2, but increased the expression levels of p-Akt, Ang1, and eNOS. In contrast, with treatment of miR-181b-5p inhibitor or Annexin V, an inhibitor of EV internalization,<sup>30</sup> Eca-109/miR-181b-5p EVs failed to induce these effects in HUVECs. Similarly, restoration of PTEN or PHLPP2 expression in EV-treated HUVECs rescued the expression of PTEN, PHLPP2, p-Akt, Ang1, Ang2, and eNOS (Figures 4D and 4E). Collectively, these results suggest that ESCC-derived EVs-miR-181b-5p suppresses the expression of PTEN and PHLPP2, and thereby activates Akt signaling in vascular endothelial cells.

#### EVs-miR-181b-5p Induces Angiogenesis to Foster ESCC Progression

To determine the effect of EVs-miR-181b-5p on ESCC progression, the KYSE30 cells mixed with EVs derived from the different transfected Eca-109 cells were subcutaneously injected into nude mice, considering that KYSE30 cells have the lowest miR-181b-5p expression level in 10 human ESCC cell lines (Figure 2D). Mice injected with Eca-109/miR-181b-5p EVs showed a high rate of tumor growth and a slow rate of weight gain. On the contrary, tumor growth was significantly slower in mice implanted with the Eca-109/inh-181b-5p EVs than in the control group (Figures 5A, 5B, and S7C–S7E). These results illustrated that EVs-miR-181b-5p promoted tumorigenicity and proliferation of tumor cells. Additionally, the levels of miR-181b-5p, PTEN, and PHLPP2 were validated in tumor tissues from each group. As expected, the Eca-109/miR-181b-5p group had a higher miR-181b-5p expression compared with the control group (Figure 5C). The protein levels of PTEN and PHLPP2 were

downregulated accordingly, whereas the mRNA levels of PTEN and PHLPP2 did not differ between each group (Figure 5D). Opposite results were obtained in the Eca-109/inh-181b-5p group (Figures 5C and 5D). Furthermore, the level of EVs-miR-181b-5p isolated from the serum of mice injected with Eca-109/miR-181b-5p EVs was significantly higher than the corresponding control group (Figure 5E). Most importantly, a lower intratumoral microvessel density was observed in tumor tissues from the Eca-109/inh-181b-5p group (Figure 5F), indicating that EVs-miR-181b-5p modulated tumor-induced angiogenesis. Inspiringly, more hepatic and pulmonary metastases were observed in mice implanted with Eca-109/miR-181b-5p EVs (Figure 5G), suggesting that EVs-miR-181b-5p contributed to ESCC metastasis.

To further confirm whether tumor-derived EVs-miR-181b-5p promotes ESCC metastasis via miR-181b-5p-induced angiogenesis, GFP-labeled KYSE30 cells were intravenously injected into nude mice, which were subsequently treated with EVs derived from the different transfected Eca-109 cells mentioned above (Figure 6A). As expected, Eca-109/miR-181b-5p EVs dramatically induced ESCC metastasis (Figure 6B). There were more hepatic and pulmonary metastatic colonies in mice injected with EVs from Eca-109/miR-181b-5p cells than those from the control group (Figures 6C, 6D, S7F, and S7G). On the contrary, Eca-109/inh-181b-5p EVs dramatically inhibited ESCC metastasis compared with the control group (Figures 6C, 6D, S7F, and S7G). Enrichment of microvessels was observed in the lung and liver metastasis induced by intravenous EVs from Eca-109/miR-181b-5p cells, as verified by CD31 expression level detected via immunohistochemistry (IHC) assay (Figures 6E and 6F). Taken together, the above results suggest that ESCC-derived EVs-miR-181b-5p regulates angiogenesis to foster tumor growth and metastasis.

#### miR-181b-5p Correlates with Angiogenesis in ESCC Patients

Tumor-derived EVs play an important role in mediating intercellular communications by transporting information cargo, which is useful for cancer diagnosis as biomarkers in circulating serum. To extend the current knowledge to ESCC patients, we first observed serum EVs collected from ESCC patients and healthy controls by electron microscopy and NanoSight particle tracking analysis (Figures 7A and 7B). Interestingly, a substantial increase of serum EV excretion was seen in ESCC patients compared with healthy controls (Figure 7B). Then we investigated EVs-miR-181b-5p expression in different serum samples (38 ESCC patients and 60 healthy controls). As shown in Figure 7C, serum EVs-miR-181b-5p expression was elevated in ESCC patients, compared with healthy controls, indicating that serum EVs-miR-181b-5p might be a potential diagnostic biomarker for ESCC patients. To further determine the correlation of miR-181b-5p expression with clinicopathological features, we

and PTEN/PHLPP2. (D) Relative luciferase activity of HUVECs in the presence of indicated treatments. (E) Migration of HUVECs was affected by miR-181b-5p in the presence of PTEN and PHLPP2 or not. Migrated cells were counted, and representative images were shown. Scale bars, 200  $\mu$ m. (F) Tube formation ability of HUVECs was affected by miR-181b-5p in the presence of PTEN and PHLPP2 or not. Branches of tubes were counted, and representative images were shown. Scale bars, 200  $\mu$ m. Experiments were performed at least in triplicate, and results are shown as mean  $\pm$  SD. Student's t test was used to analyze the data (\*p < 0.05; \*\*p < 0.01; \*\*\*p < 0.001).

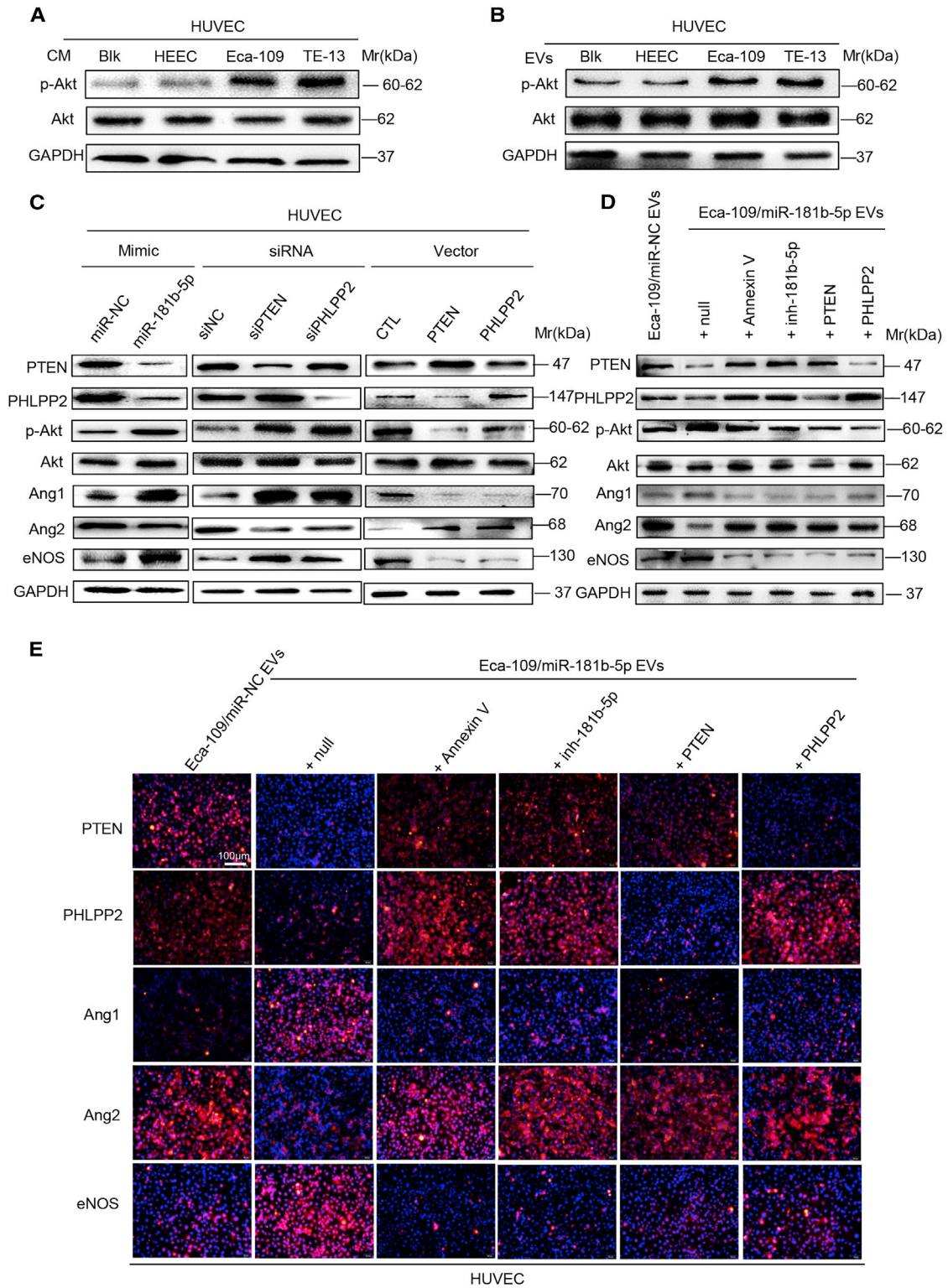


**Figure 4. EVs-miR-181b-5p Regulates Angiogenesis via the Akt Signaling Pathway**

(A) The expression of indicated proteins in HUVECs treated with CM from HEEC and ESCC cell lines was detected by western blot. (B) The expression of indicated proteins in HUVECs treated with EVs from HEEC and ESCC cell lines was detected by western blot. (C) The expression of indicated proteins in HUVECs treated with miR-181b-5p

(legend continued on next page)

performed *in situ* hybridization (ISH) of 87 human ESCC tissue samples and confirmed that miR-181b-5p expression was elevated in ESCC tissues compared with normal tissues (Figure 7D). The ESCC tissue samples were divided into two groups (high and low) according to the scores of miR-181b-5p expression level. As shown in Figure 7E, high miR-181b-5p expression was well predicted for poor overall survival (OS). In addition, it was detected that high miR-181b-5p expression was correlated with high advanced N stage and clinical stage (N stage,  $p = 0.000$ ; clinical stage,  $p = 0.000$ ; Table S3). In addition, multivariate analysis indicated that miR-181b-5p expression (hazard ratio [HR], 0.423; 95% confidence interval [CI], 0.215–0.831;  $p = 0.012$ ) was an independent prognostic factor for OS in ESCC patients (Table S4). Taken together, these data showed that miR-181b-5p is highly expressed in ESCC tissues and serum EVs. Moreover, high miR-181b-5p expression level in ESCC patients predicted poor outcome. To further confirm the correlation between miR-181b-5p expression and microvessel density in ESCC, we performed ISH of miR-181b-5p in combination with IHC staining of vascular endothelial cell markers (CD31) on serial sections of human ESCC tissues and adjacent normal tissues. As shown in Figures 7F and 7G, miR-181b-5p signals were present in both tumor cells and vascular endothelial cells around the tumor, and CD31 was strongly positively correlated with miR-181b-5p, indicating that miR-181b-5p correlates with angiogenesis in ESCC patients.

## DISCUSSION

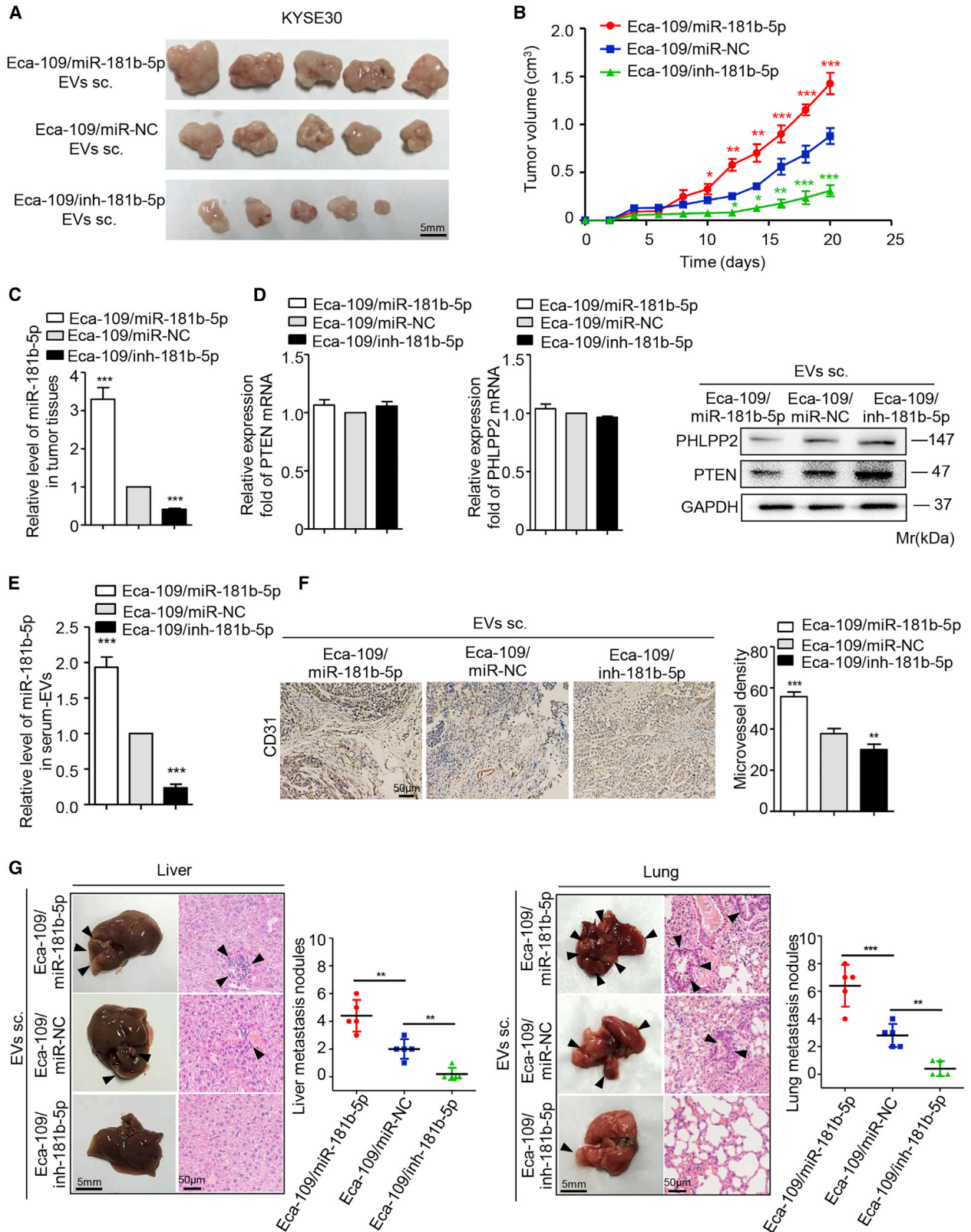
Tumor microenvironment, a dynamic system orchestrated by intercellular communications, is responsible for tumor progression and metastasis.<sup>31</sup> It necessitates the study of the interaction between tumor and vascular endothelial cells mediated by EVs. In our study, we provide a novel insight on the mechanism that ESCC-derived EVs-miR-181b-5p reprograms endothelial cells in the tumor microenvironment, primarily inducing angiogenesis by decreasing its targets PTEN and PHLPP2 expression to activate the Akt signaling pathway. Subsequently, rich vascular anastomoses further facilitate ESCC tumorigenesis by supplying oxygen and nutrients, and foster tumor metastasis by serving as a conduit (Figure 7H), which is one of the reasons that tumor-derived EVs-miR-181b-5p facilitates ESCC tumorigenesis and metastasis. However, these effects are multi-factorial and not solely presented as a result of altered angiogenesis. It has been reported that tumor-derived EVs maintain cancer stem-like cell dynamic equilibrium, facilitate the epithelial-mesenchymal transition, and induce PD1<sup>+</sup> tumor-associated macrophages expansion in esophageal carcinoma.<sup>32–34</sup> Moreover, miR-181b was reported to promote cell autophagy and restrain cell apoptosis by regulating the CREBRF/CREB3 pathway in gallbladder carcinoma.<sup>35</sup> In addition, miR-181b-5p could regulate the expression of proteins associated with cell migration, including TIMP-3 and annexin A2.<sup>36</sup> Therefore, more potential mechanisms deserve further investigation.

Previous studies have reported that miR-181b-5p is expressed aberrantly in several cancers. For example, astrocytoma shows high expression of miR-181b-5p, which is significantly associated with poor patient survival.<sup>37</sup> It is also determined that miR-181b-5p is upregulated in serum of acute myeloid leukemia (AML) patients compared with healthy controls.<sup>38</sup> To the contrary, miR-181b-5p is significantly downregulated and acts as a tumor suppressor in astrocytoma.<sup>39</sup> However, few studies have reported the biological functions of miR-181b-5p in tumor progression. Our data demonstrate that ESCC-derived EVs-miR-181b-5p modulates vascular endothelial cells to secrete Ang1 and eNOS, which contributes to tumor angiogenesis. Moreover, EVs-miR-181b-5p facilitates tumor growth and has a positive correlation with ESCC metastasis. In addition, miR-181b-5p is highly expressed in ESCC tissues and serum EVs, and high miR-181b-5p expression in ESCC patients predicts a poor outcome, which holds important implications for efficient prevention and therapeutic strategies. As diverse substances are contained in EVs, the role of EVs in cancer remains to be thoroughly studied. Even so, treatments targeting EVs provide meaningful opportunities for tumor therapeutic strategies. According to the above results, future work will be required to focus on the role of EVs-miR-181b-5p in the clinic.

Bioinformatics data predict that PTEN and PHLPP2 are the direct targets of miR-181b-5p, which are well-known tumor suppressors due to their ability to block the Akt signaling pathway in several cancer cells.<sup>40,41</sup> Herein, we detected Akt expression and downstream signaling in our experiment models. Vascular morphogenesis and homeostasis are complex biological processes that are tightly controlled by multiple signaling pathways. Among them, the Ang/Tie2 signaling pathway has received more and more attention in the past decade. Ang1 activates Tie2 and accelerates vascular endothelial cells survival, migration, and sprouting, resulting in stabilization and maturation of blood vessels.<sup>42</sup> Ang2 acts as a Tie2 antagonist to destabilize the established vasculature by inhibiting Ang1-induced Tie2 phosphorylation.<sup>43</sup> It has been reported that activation of Akt signaling negatively regulates Ang2 and promotes the angiogenic process.<sup>44</sup> In addition, NO, which is synthesized by eNOS, induces vasodilation and increases vascular permeability. Activation of the Akt signaling pathway promotes eNOS phosphorylation and NO release.<sup>45</sup> Moreover, it is reported that Ang2 can be inhibited by the Akt/eNOS signaling pathway.<sup>46</sup> Therefore, the role of Akt signaling in the activation of Ang2 and eNOS signaling induced by EVs-miR-181b-5p seems worthy of investigating. Our results show that ESCC-derived EVs-miR-181b-5p suppresses the expression level of Ang2 but increases the expression levels of Ang1 and eNOS in vascular endothelial cells to promote cancer-induced angiogenesis via Akt signaling and downstream signaling activation.

---

mimic, siRNA of PTEN/PHLPP2, or control was detected by western blot. (D) The expression of indicated proteins in HUVECs incubated with Eca-109/miR-NC EVs, Eca-109/miR-181b-5p EVs, Eca-109/miR-181b-5p EVs + Annexin V, Eca-109/miR-181b-5p EVs + inh-181b-5p, Eca-109/miR-181b-5p EVs + PTEN, or Eca-109/miR-181b-5p EVs + PHLPP2 was detected by western blot. (E) The expression of indicated proteins was detected by immunofluorescence. Representative images were shown. Scale bar, 100  $\mu\text{m}$ . Experiments were performed at least in triplicate.



(legend on next page)

In conclusion, our results indicate that ESCC-derived EVs-miR-181b-5p modulates vascular endothelial cells by decreasing PTEN and PHLPP2, which activates the Akt signaling pathway to promote intratumoral microvessel formation. Furthermore, rich vascular anastomoses facilitate ESCC progression and metastasis. More importantly, high miR-181b-5p expression in tissues and serum EVs shows a positive correlation with poor prognosis in ESCC patients. Our study elucidates a new molecular mechanism underlying the crosstalk between tumor cells and vascular endothelial cells to foster a vascular-rich microenvironment and tumor progression, which contribute to efficient prevention and therapeutic strategies for ESCC.

## MATERIALS AND METHODS

### Tissue and Serum Specimens

Two independent cohorts comprising 145 ESCC patients were enrolled for this study. In cohort 1, ESCC and adjacent nontumor specimens were gathered from 58 patients who were diagnosed with ESCC between December 2014 and November 2015 in Nanjing General Hospital of Nanjing Military Command (Jiangsu, China). The study was approved by Nanjing General Hospital of Nanjing Military Command Review Board. In cohort 2, paraffin-embedded tissue samples were collected from archival materials stored in the Biobank Center at the National Engineering Center for Biochip at Shanghai (Shanghai Outdo Biotech). Specimens from ESCC and adjacent nonmalignant tissues were collected from 87 ESCC patients who underwent surgical resection between 2009 and 2010, and were followed up for 6.5 years. The clinical characteristics of all patients are listed in Tables S2 and S3. In addition, human serum specimens were collected from 38 ESCC patients and 60 healthy donors before resection in the Jiangsu Province Hospital (Nanjing, China). Informed consent was obtained from all participants. All patients were diagnosed according to the guidelines of the American Joint Commission on Cancer and the guidelines of the International Union Against Cancer (IUAC). The study was conducted in accordance with the Ethics Committee of China Pharmaceutical University.

### miRNA Microarray

miRNA microarray analysis was undertaken using the above seven paired samples of ESCC versus adjacent noncancerous tissues (Nanjing General Hospital of Nanjing Military Command). In brief, miRNAs were extracted and purified from total RNA using a mirVana miRNA Isolation Kit (Ambion). A poly(A) tail labeled with biotin labeling 3DNA dendrimer (FlashTag Biotin RNA Labeling) was added in the 3' end of miRNA using poly(A) polymerase. Biotin-labeled miRNA hybridized to the Affymetrix GeneChip

miRNA Array 4.0. Array (Affymetrix) was scanned with a GeneChip Scanner 3000, and the images were processed using the AGCC software (Affymetrix GeneChip Command Console Software). Signals were normalized by the median center tool for genes in the Cluster 3.0 software and analyzed by significance analysis of microarrays (SAM), with the false discovery rate (FDR) threshold set at 0 and fold change set (fold change  $\geq 2.5$ ,  $p \leq 0.001$  or fold change  $\leq -2.5$ ,  $p \leq 0.001$ ). The microarray data were published in NCBI Gene Expression Omnibus and are accessible through GEO: GSE97049.

### Cell Culture

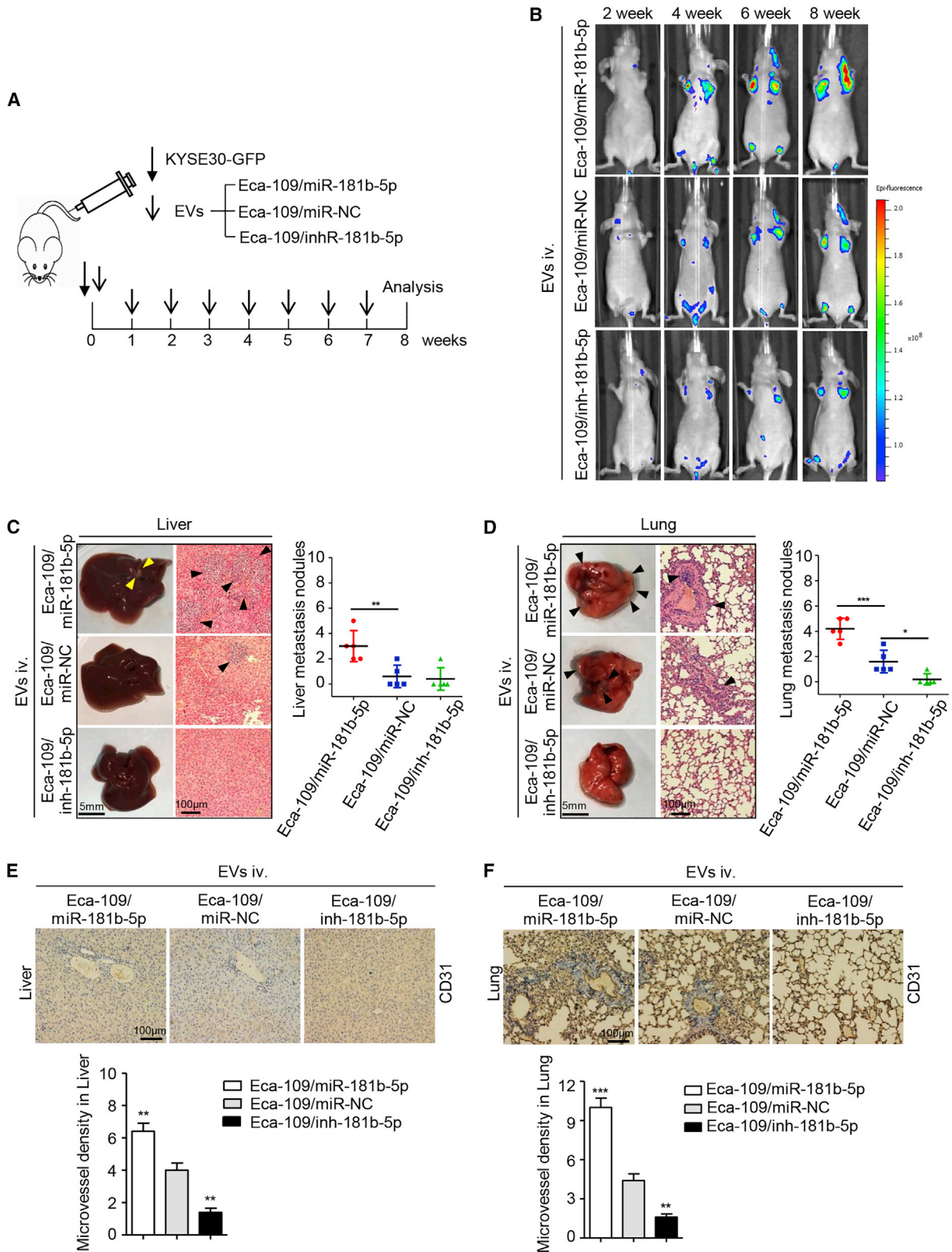
The human ESCC cell lines (TE-10, TE-12, TE-13, Eca-109, KYSE-30, KYSE-150, KYSE-180, KYSE-410, KYSE-450, KYSE-510) and normal HEEC lines were kindly supplied by Prof. Yifeng Zhou, Suzhou University, in 2015. All cell lines were cultured in RPMI 1640 (GIBCO, USA) medium containing 10% FBS (BI, Israel) or 10% exosome-free serum (VivaCell, China). ESCC cells were authenticated by short tandem repeats (STRs) profiling and confirmed to be mycoplasma negative. HUVECs were cultured in endothelial cell medium (ECM) medium (ScienCell Research Laboratories, USA) containing 10% FBS (BI, Israel) or 10% exosome-free serum (VivaCell, China) and 1% endothelial cell growth supplement (ECGS) (ScienCell Research Laboratories, USA). For co-culture, ESCC cells were seeded in the upper Transwell chambers, and HUVECs were seeded in the lower 24-well plates. EV secretion inhibitor GW4869 (10 mM; Sigma-Aldrich, USA) was added to the upper Transwell chambers, and cells were co-cultured for 24 h. All cell lines were cultivated at 37°C in 5% CO<sub>2</sub> humidified atmosphere.

### Reagents and Antibodies

Antibodies for TSG101 (14497-1-AP, 1:1,000), HSP70 (10995-1-AP, 1:1,000), Angiopoietin 1 (23302-1-AP, 1:1,000), Angiopoietin 2 (24613-1-AP, 1:1,000), PHLPP2 (25244-1-AP, 1:1,000), and p-Akt (66444-1-Ig, 1:3,000) were purchased from Sanying (China). Antibodies for Akt (WL0003b, 1:500), eNOS (WL0992a, 1:500), PTEN (WL01901, 1:500), and CD63 (WL02549, 1:1,000) were purchased from Wanlei (China). Antibodies for GRP94 (D120724, 1:1,000) were purchased from BBI (China). Antibodies for CD9 (ab92726, 1:2,000) were purchased from Abcam (USA). Antibodies for GAPDH (70-ab011-040, 1:2,000) served as a reference protein probe, and HRP-conjugated Goat Anti-Rabbit IgG (70-GAR007, 1:1,000) was purchased from Multisciences (China). Cy3-AffiniPure Goat Anti-Rabbit IgG was purchased from Yeasen (China). Annexin V was purchased from BD Biosciences (USA).

### Figure 5. EVs-miR-181b-5p Induces Angiogenesis to Foster ESCC Tumorigenicity and Proliferation *In Vivo*

(A and B) Xenograft assays of KYSE30 cells mixed with EVs derived from Eca-109/miR-181b-5p cells, Eca-109/inh-181b-5p cells, or Eca-109/miR-NC cells were performed on nude mice ( $n = 5$ ). Representative tumors (A) and tumor growth curves (B) were shown. Scale bar, 5 mm. (C) The expression of miR-181b-5p in tumor tissues was determined by quantitative relative real-time PCR. (D) The expression of PTEN and PHLPP2 in tumor tissues was determined by quantitative relative real-time PCR and western blot. (E) The expression of miR-181b-5p in serum EVs was determined by quantitative relative real-time PCR. (F) The tumor tissues were performed by immunohistochemistry staining for CD31, and microvessel density was analyzed. Representative micrographs were shown. Scale bar, 50  $\mu$ m. (G) The number of liver and lung metastatic sites (indicated by arrowheads) was determined by H&E staining and counted under the microscope. Scale bars, 5 mm (G, right panels); 50  $\mu$ m (F and G, left panels). Each experiment was performed in triplicate, and data are presented as mean  $\pm$  SD. Student's *t* test was used to analyze the data (\* $p < 0.05$ ; \*\* $p < 0.01$ ; \*\*\* $p < 0.001$ ).



(legend on next page)

### Western Blotting

Tissue, cell, and EV lysates were homogenized in radio-immunoprecipitation assay (RIPA) buffer (KeyGEN BioTECH, China) and quantified using bicinchoninic acid (BCA) assay. After immunoblotting, the proteins were transferred onto polyvinylidene fluoride (PVDF) membranes (Millipore, USA), which were subsequently incubated with primary antibodies overnight at 4°C. Following incubation with the specific HRP-conjugated Goat Anti-Rabbit IgG, chemiluminescence signal was detected using BeyoECL Plus (Beyotime, China). Protein expression was normalized to the GAPDH level.

### Isolation and Analysis of EVs

For EV isolation, ESCC cells were cultured in RPMI 1640 medium containing 10% exosome-free serum. The culture medium (CM) was collected and filtrated through 0.22- $\mu$ m filters (Millipore, USA). EVs in CM or serum samples were isolated by ultracentrifugation according to the standard method. First, samples were centrifuged at  $10,000 \times g$  for 10 min to remove the other debris; then the supernatant was collected and centrifuged at  $100,000 \times g$  for 70 min to pellet EVs. Ultracentrifugation experiments were performed with Optima L-80XP (Beckman Coulter, USA). BCA assay was performed to measure the protein concentrations in EVs. For nanoparticle tracking analysis, the size and number of EVs were detected by ZetaView (Microtrac, USA). For transmission electron microscopy observation, 10  $\mu$ g EVs was dropped to carbon-coated Cu grids and baked for 5 min under infrared light. EV samples were then negatively stained with 3% (w/v) aqueous phosphotungstic acid for 5 min. The embedded samples were observed under HT7700 transmission electron microscope (Hitachi, Japan).

### EVs Tracing

EVs were labeled using PKH26 Red Fluorescent Cell Linker Kits (Sigma-Aldrich, USA) according to the manufacturer's instruction and then washed with PBS twice. PKH26-labeled EVs were collected by ultracentrifugation at  $100,000 \times g$  for 70 min and then co-cultured with HUVECs for 1.5 h. Subsequently, HUVECs were fixed and stained with Hoechst. The cells and EVs were visualized under confocal laser scanning microscopy (Carl Zeiss, Germany).

### Gene Knockdown or Overexpression

For transient transfection, HUVECs were transfected with a miR-181b-5p mimic, an inhibitor, or a negative control (Applied Biological Materials, Canada), respectively. HUVECs were transfected with siRNAs targeting PTEN, PHLPP2, or a negative control RNA duplex (GenePharma, China) using Lipofectamine 3000 (Invitrogen, USA)

according to the manufacturer's instructions. The siRNA sequences were listed in Table S5. For stable transfection, Eca-109 cells were transfected with a miRCURY LNA miR-181b-5p mimic, an inhibitor, or a negative control (Exiqon, Denmark), respectively. For overexpression, the full-length complementary DNAs (cDNAs) of PTEN and PHLPP2 were synthesized and cloned into the lentiviral expression vector of pLenti-GIII-CMV-GFP-2A-Puro (Applied Biological Materials, Canada), whereas an empty lentiviral vector was used as a control. The lentiviral vector HUBLV-GFP-Puro-Luc (HANBIO, China) was cloned into Eca-109 cells for tail vein metastasis assay. Transfected cells were selected with 1  $\mu$ g/mL puromycin for 2 weeks. The transfection efficiency was monitored by the GFP.

### RNA Extraction and Quantitative Reverse Transcriptase PCR

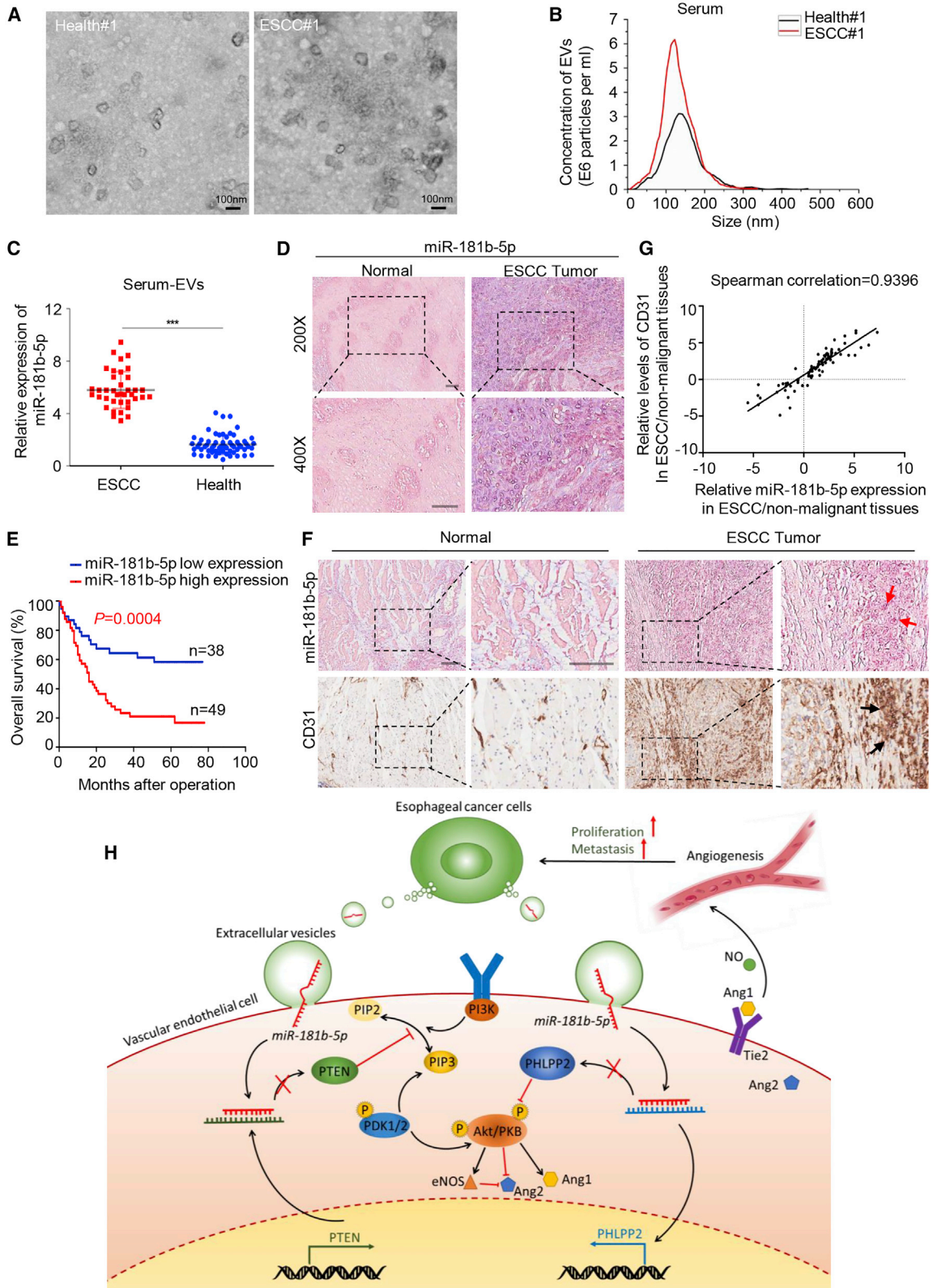
Total RNA was extracted from tissues or cells with TRIzol reagent (Invitrogen, USA), and RNA from EVs in CM or serum was extracted with the exoRNeasy Serum/Plasma Midi Kit (QIAGEN, Germany) according to the manufacturer's instructions. Reverse transcription reaction was performed using PrimeScript RT reagent Kit (Takara, China). Quantitative relative real-time PCR was measured using a SYBR Premix Ex Taq II Kit (Takara, China) by QuantStudio 3 Real-Time PCR System (Applied Biosystems, USA). The quantity of specific mRNA was calculated according to the cycle threshold (CT) values, which were normalized to the housekeeping gene (GAPDH). poly(A) addition to miRNA and reverse transcription reaction were performed using miRNA cDNA Synthesis Kit (Applied Biological Materials, Canada). The BrightGreen miRNA qPCR MasterMix Kit (Applied Biological Materials, Canada) was used to quantify the relative abundance of miR-181b-5p. Relative expression levels of miRNA were normalized to U6 or miR-39 expression. The specific primer sequences were listed in Table S5.

### Tube Formation Assay, Migration Assay, and Wound Healing Assay

For tube formation assay, 96-well plates were coated with 50  $\mu$ L Matrigel (BD Biosciences, USA) and incubated at 37°C for polymerization. A total of  $1.5 \times 10^4$  HUVECs were seeded on the Matrigel-coated well with 100  $\mu$ L ECM completed medium. For EV function detection, equal quantities of tumor-derived EVs were added into the plates. The plates were then incubated at 37°C in 5% CO<sub>2</sub> for 6 h. Tube formation was observed under a microscope (Olympus, Japan). For migration assay,  $5 \times 10^3$  HUVECs or ESCC cells were seeded on the upper Transwell chamber in serum-free ECM medium. ECM with 10% exosome-free serum was added to the lower 24-well

### Figure 6. EVs-miR-181b-5p Induces Angiogenesis to Foster ESCC Metastasis *In Vivo*

(A) The flow diagram for creating the metastatic tumor model. (B) Representative images of liver and lung metastasis of indicated mice treated with EVs derived from Eca-109/miR-181b-5p cells, Eca-109/miR-NC cells, or Eca-109/inh-181b-5p cells were determined by GFP-based fluorescence imaging ( $n = 5$ ). (C) The number of liver metastatic sites (indicated by arrows) was determined by H&E staining and counted under microscope. Scale bars, 5 mm (left panels); 100  $\mu$ m (right panels). (D) The number of lung metastatic sites (indicated by arrows) was determined by H&E staining and counted under microscope. Scale bars, 5 mm (left panels); 100  $\mu$ m (right panels). (E) The livers were performed by immunohistochemistry staining for CD31, and microvessel density was analyzed. Scale bars, 100  $\mu$ m. (F) The lungs were performed by immunohistochemistry staining for CD31, and microvessel density was analyzed. Scale bars, 100  $\mu$ m. Each experiment was performed three times independently, and data are presented as mean  $\pm$  SD. Student's t test was used to analyze the data (\* $p < 0.05$ ; \*\* $p < 0.01$ ; \*\*\* $p < 0.001$ ).



(legend on next page)

plates. Equal quantities of tumor-derived EVs were added into the inserts to detect EV function. After cultivation at 37°C for 24 h, the migrated cells were fixed by ethanol after washing by PBS and stained by crystal violet. Representative fields were photographed under microscope, and the number of migrated cells per field was counted. For wound healing assay,  $3 \times 10^4$  HUVECs were seeded on 96-well plates. Each well was scraped with a 10- $\mu$ L pipette tip to create two linear regions devoid of cells. After being treated with tumor-derived EVs for 24 h, HUVECs that migrated into the cleared section were observed under a microscope at specific time points. Each experiment was repeated three times.

#### Cell Viability Assay and Cell-Cycle Assay

For cell viability assay,  $1 \times 10^4$  HUVECs were seeded on 96-well plates and cultured in ECM containing 10% exosome-free serum. After being treated with tumor-derived EVs for 12 h, cell proliferation was measured by the Cell Counting Kit-8 (Dojindo, Japan) at 0, 24, 48, and 72 h according to the manufacturer's instructions. For cell-cycle assay,  $1 \times 10^6$  HUVECs were fixed in 70% ethanol at 4°C overnight and then stained with propidium iodide (PI) using cell-cycle assay kit (BD Biosciences, USA) according to the manufacturer's instructions. Cell-cycle analysis was measured by the CytoFLEX Flow Cytometer (Beckman Coulter, USA). The data were analyzed using FlowJo 10.0 software.

#### In Vivo Matrigel Plug Assay

A total of 20  $\mu$ g EVs that derived from ESCC cells was mixed with Matrigel (BD Biosciences, USA) and subcutaneously injected into BALB/c athymic nude mice 6–8 weeks old. After 14 days, the Matrigel plugs were harvested and stained by hematoxylin and eosin (H&E). Immunohistochemical staining for CD31 (Abcam, USA) was also performed. The expression of CD31 mRNA was determined by quantitative relative real-time PCR. ImageJ software was used to analyze the vessel area.

#### Animal Studies

Six-week-old female BALB/c athymic nude mice were purchased from the Laboratory Animal Center of Yangzhou University (Yangzhou, China). The procedure of all animal experiments complied with Institutional Animal Care and Use Committee (IACUC) regulations. All animal experiments were approved by the Ethics Committee of China Pharmaceutical University Permit Number SYXK2016-0011. BCA assay was performed to measure the protein concentrations in EVs. For tumor xenograft assay, a total of  $5 \times 10^6$  KYSE30 cells mixed

with 40  $\mu$ g EVs derived from Eca-109/miR-181b-5p cells, Eca-109/inh-181b-5p cells, or Eca-109/miR-NC cells were injected subcutaneously into BALB/c athymic nude mice. After 20 days, mice were sacrificed to remove the xenografted tumors, and the volumes and weights of the tumors were recorded. Immunohistochemical staining for CD31 was used to observe angiogenesis in tumor tissues. Metastatic lesions in livers and lungs were observed by H&E staining. Quantitative relative real-time PCR was used to detect miR-181b-5p expression in tumor tissues or EVs from mice serum. For tail vein metastasis assay,  $1 \times 10^6$  GFP-labeled KYSE30 cells were intravenously injected into female BALB/c athymic nude mice through the tail vein. Subsequently, mice were divided into groups randomly and intravenously injected with 20  $\mu$ g EVs from the transfected Eca-109 cells once a week for 2 months. Hepatic and pulmonary metastasis was observed by *ex vivo* bioluminescent imaging using IVIS Lumina series III (PerkinElmer, USA) once a week. After 2 months, mice injected with EVs were sacrificed, whereas livers and lungs were removed for examination. H&E staining and immunohistochemical staining for CD31 were used to observe metastatic lesions and vessels.

#### Luciferase Reporter Assay

To identify the binding site between miR-181b-5p and PTEN/PHLPP2, HUVECs were transfected with a luciferase construct containing PTEN and PHLPP2 with the wild-type or a mutated version of the binding site, and co-transfected with a miR-181b-5p mimic or an empty vector. For evaluating the luciferase activities of PTEN and PHLPP2, HUVECs were pre-treated with tumor-derived EVs for 24 h and then transfected with a luciferase vector containing PTEN and PHLPP2 with the wild-type or a mutated version of the binding site. The luciferase vectors were constructed by GenePharma (Shanghai, China). After transfection, the Dual Luciferase kit (Promega, USA) was used to detect the luciferase activities according to the manufacturer's instructions.

#### ISH

The double-digoxin (DIG)-labeled miRCURY LNA microRNA ISH Detection Probe (Exiqon, Denmark) was employed for visualization of the miR-181b-5p. ISH of miR-181b-5p with ESCC tissue microarrays (TMAs) was performed by Shanghai Outdo Biotech (catalog no. HEso-Squ180Sur-03). There were 87 human ESCC tissue samples with information of OS times and clinicopathological characteristics in these TMAs. The tissue array was stained with H&E to verify the presence of cells.

#### Figure 7. miR-181b-5p Correlates with Angiogenesis in ESCC Patients

(A) EVs in serum from ESCC patients and healthy controls were observed by electron microscopy. Scale bar, 100 nm. (B) The concentration of EVs in serum was detected by NanoSight particle tracking analysis. (C) miR-181b-5p expression in serum EVs from healthy donors and ESCC patients was detected by quantitative relative real-time PCR. Data are presented as mean  $\pm$  SD. Student's t test was used to analyze the data (\*\*p < 0.001). (D) *In situ* hybridization (ISH) of miR-181b-5p with ESCC tissue microarrays (TMAs) was performed to detect miR-181b-5p expression in normal and tumor tissues. Representative images were shown. Scale bar, 50  $\mu$ m. (E) Kaplan-Meier plots of overall survival of 87 patients with ESCC, stratified by expression of miR-181b-5p. Survival data were analyzed by the Kaplan-Meier method and log rank test. (F) ISH of miR-181b-5p in combination with IHC staining of endothelial cell markers (CD31) on serial sections of human ESCC tissues and adjacent normal tissues. Scale bar, 100  $\mu$ m. (G) The correlation between CD31 and miR-181b-5p in ESCC tissues using Spearman's test. (H) Proposed schematic diagram of tumor-derived EVs-miR-181b-5p mediating angiogenesis to promote ESCC progression and metastasis.

The sections were deparaffinized, digested by proteinase K, hydrated, and deproteinated. Then the sections were prehybridized in hybridization buffer for 2 h in a humidified chamber at 55°C. Hybridization was performed by applying 20 nM probe in hybridization buffer to the array slides covered with Nescofilm (Bando Chemical, Japan) overnight at 55°C in a humidified chamber. Hybridized probes were visualized by incubation with anti-digoxigenin and alkaline phosphatase conjugate at 37°C for 30 min, followed by nitro blue tetrazolium/5-bromo-4-chloro-3-indolyl-phosphate to develop a blue color. Finally, the cells were counter-stained with nuclear fast red for 3–5 min and mounted on slides. Sections with 5% labeled cells were scored as 0, sections with 5%–30% labeled cells were scored as 1, sections with 31%–70% labeled cells were scored as 2, and sections in excess of 71% labeled cells were scored as 3. The staining intensity was scored similarly, with 0 indicating negative staining, 1 indicating weakly positive staining, 2 indicating moderately positive staining, and 3 indicating strongly positive staining. The scores for the percentage of positive tumor cells and staining intensity were summed to generate an immunoreactive score for each specimen. A final score of 0–1 indicated negative expression (–), 2–3 indicated weak expression (+), 4–5 indicated moderate expression (++), and 6 indicated strong expression (+++). Images were captured with Aperio ScanScope CS2 (Aperio, USA) and assessed with ImageScope software (Aperio, USA).

### IHC and Immunofluorescence

For IHC analysis, the slides of tumors, Matrigel plugs, livers, and lungs were incubated with CD31 primary antibodies, which was followed by incubation with horseradish peroxidase-conjugated secondary antibodies (Santa Cruz Biotechnology, USA). Finally, the staining processes were performed with diaminobenzidine colorimetric reagent solution (Dako, USA) and hematoxylin (Sigma-Aldrich, USA). Images were taken to evaluate CD31 expression using Pro Plus software. For immunofluorescence observation, HUVECs were fixed with 4% paraformaldehyde at room temperature for 30 min and permeabilized with 0.1% Triton X-100. Staining was performed with primary antibodies mentioned above, which was followed by incubation with Cy3-AffiniPure Goat Anti-Rabbit IgG. Hoechst was used to label the cell nucleus. All samples were observed using a fluorescence microscope (Olympus, Japan).

### Statistics Analysis

Data analysis was performed using SPSS Statistics 25.0. The paired t test was performed to detect the differential expression of miR-181b-5p in cancer tissues compared with adjacent nonmalignant tissues. The relationship between miR-181b-5p and clinicopathological characteristics was evaluated using chi-square test. Survival curves were calculated using Kaplan-Meier and log rank tests. The effects of variables on survival were analyzed by univariate and multivariate Cox proportional hazards modeling. Two-group comparison, multiple-group comparison, and correlation analyses were calculated with a paired two-tailed Student's t test, two-way ANOVA test, linear regression test, and Pearson's test using GraphPad Prism 5 software (GraphPad Software, USA), respectively. The p values less than 0.05

were considered statistically different (\*p < 0.05; \*\*p < 0.01; \*\*\*p < 0.001).

### SUPPLEMENTAL INFORMATION

Supplemental Information can be found online at <https://doi.org/10.1016/j.omtn.2020.03.002>.

### AUTHOR CONTRIBUTIONS

Y.W., J.L., and L.C. performed most of the experiments, analyzed the data, and wrote the manuscript. H.B., D.L., and C.X. performed some of the experiments. Y.W., J.L., and J.H. reviewed and edited the manuscript. H.X. and Y.W. designed the experiments and edited the manuscript. H.X. is the guarantor of this work, has full access to all data reported in the study, and takes responsibility for the integrity of the data and the accuracy of the data analysis.

### CONFLICTS OF INTEREST

The authors declare no competing interests.

### ACKNOWLEDGMENTS

This work was supported by grants from the Project Program of State Key Laboratory of Natural Medicines (SKLNMZZCX201821) and the National Science and Technology Major Projects of New Drugs (2018ZX09301053-001, 2018ZX09301039-002, and 2018ZX09201001-004-001) in China. This work was also supported by the Priority Academic Program Development of Jiangsu Higher Education Institutions (PAPD), China Postdoctoral Science Foundation (2017M621884), and “Double First-Class” University project of China Pharmaceutical University (grants CPU2018GY13 and CPU2018PZH03). The funders had no role in study design; in collection, analysis, or interpretation of the data; in the writing of the report; or in the decision to submit this article for publication.

### REFERENCES

- Rustgi, A.K., and El-Serag, H.B. (2014). Esophageal carcinoma. *N. Engl. J. Med.* *371*, 2499–2509.
- Murphy, G., McCormack, V., Abedi-Ardekani, B., Arnold, M., Camargo, M.C., Dar, N.A., Dawsey, S.M., Etemadi, A., Fitzgerald, R.C., Fleischer, D.E., et al. (2017). International cancer seminars: a focus on esophageal squamous cell carcinoma. *Ann. Oncol.* *28*, 2086–2093.
- Taylor, P.R., Abnet, C.C., and Dawsey, S.M. (2013). Squamous dysplasia—the precursor lesion for esophageal squamous cell carcinoma. *Cancer Epidemiol. Biomarkers Prev.* *22*, 540–552.
- Arnold, M., Soerjomataram, I., Ferlay, J., and Forman, D. (2015). Global incidence of oesophageal cancer by histological subtype in 2012. *Gut* *64*, 381–387.
- Dotto, G.P., and Rustgi, A.K. (2016). Squamous cell cancers: a unified perspective on biology and genetics. *Cancer Cell* *29*, 622–637.
- Weis, S.M., and Cheresh, D.A. (2011). Tumor angiogenesis: molecular pathways and therapeutic targets. *Nat. Med.* *17*, 1359–1370.
- Dimova, I., Popivanov, G., and Djonov, V. (2014). Angiogenesis in cancer - general pathways and their therapeutic implications. *J. BUON* *19*, 15–21.
- Chen, Y., Wang, D., Peng, H., Chen, X., Han, X., Yu, J., Wang, W., Liang, L., Liu, Z., Zheng, Y., et al. (2019). Epigenetically upregulated oncoprotein PLCE1 drives esophageal carcinoma angiogenesis and proliferation via activating the PI-PLCε-NF-κB signaling pathway and VEGF-C/ Bcl-2 expression. *Mol. Cancer* *18*, 1–19.

9. Small, H.Y., Montezano, A.C., Rios, F.J., Savoia, C., and Touyz, R.M. (2014). Hypertension due to antiangiogenic cancer therapy with vascular endothelial growth factor inhibitors: understanding and managing a new syndrome. *Can. J. Cardiol.* *30*, 534–543.
10. Cocucci, E., and Meldolesi, J. (2015). Exosomes and exosomes: shedding the confusion between extracellular vesicles. *Trends Cell Biol.* *25*, 364–372.
11. Milane, L., Singh, A., Mattheolabakis, G., Suresh, M., and Amiji, M.M. (2015). Exosome mediated communication within the tumor microenvironment. *J. Control. Release* *219*, 278–294.
12. Zeng, Z., Li, Y., Pan, Y., Lan, X., Song, F., Sun, J., Zhou, K., Liu, X., Ren, X., Wang, F., et al. (2018). Cancer-derived exosomal miR-25-3p promotes pre-metastatic niche formation by inducing vascular permeability and angiogenesis. *Nat. Commun.* *9*, 5395–5409.
13. Lin, X.J., Fang, J.H., Yang, X.J., Zhang, C., Yuan, Y., Zheng, L., and Zhuang, S.M. (2018). Hepatocellular carcinoma cell-secreted Exosomal MicroRNA-210 promotes angiogenesis in vitro and in vivo. *Mol. Ther. Nucleic Acids* *11*, 243–252.
14. Kourembanas, S. (2015). Exosomes: vehicles of intercellular signaling, biomarkers, and vectors of cell therapy. *Annu. Rev. Physiol.* *77*, 13–27.
15. Hayes, J., Peruzzi, P.P., and Lawler, S. (2014). MicroRNAs in cancer: biomarkers, functions and therapy. *Trends Mol. Med.* *20*, 460–469.
16. Stark, A., Brennecke, J., Bushati, N., Russell, R.B., and Cohen, S.M. (2005). Animal MicroRNAs confer robustness to gene expression and have a significant impact on 3'UTR evolution. *Cell* *123*, 1133–1146.
17. Ambros, V. (2004). The functions of animal microRNAs. *Nature* *431*, 350–355.
18. Bartel, D.P. (2004). MicroRNAs: genomics, biogenesis, mechanism, and function. *Cell* *116*, 281–297.
19. Fiedler, J., and Thum, T. (2016). New Insights Into miR-17-92 Cluster Regulation and Angiogenesis. *Circ. Res.* *118*, 9–11.
20. Mao, G., Liu, Y., Fang, X., Liu, Y., Fang, L., Lin, L., Liu, X., and Wang, N. (2015). Tumor-derived microRNA-494 promotes angiogenesis in non-small cell lung cancer. *Angiogenesis* *18*, 373–382.
21. Sasahira, T., Kurihara, M., Bhawal, U.K., Ueda, N., Shimamoto, T., Yamamoto, K., Kiritani, T., and Kuniyasu, H. (2012). Downregulation of miR-126 induces angiogenesis and lymphangiogenesis by activation of VEGF-A in oral cancer. *Br. J. Cancer* *107*, 700–706.
22. Geng, L., Chaudhuri, A., Talmon, G., Wisecarver, J.L., Are, C., Brattain, M., and Wang, J. (2014). MicroRNA-192 suppresses liver metastasis of colon cancer. *Oncogene* *33*, 5332–5340.
23. Wang, R., Zhao, N., Li, S., Fang, J.H., Chen, M.X., Yang, J., Jia, W.H., Yuan, Y., and Zhuang, S.M. (2013). MicroRNA-195 suppresses angiogenesis and metastasis of hepatocellular carcinoma by inhibiting the expression of VEGF, VAV2, and CDC42. *Hepatology* *58*, 642–653.
24. Chou, J., Lin, J.H., Brenot, A., Kim, J.W., Provot, S., and Werb, Z. (2013). GATA3 suppresses metastasis and modulates the tumour microenvironment by regulating microRNA-29b expression. *Nat. Cell Biol.* *15*, 201–213.
25. Park, J.K., Peng, H., Yang, W., Katsnelson, J., Volpert, O., and Lavker, R.M. (2017). miR-184 exhibits angiostatic properties via regulation of Akt and VEGF signaling pathways. *FASEB J.* *31*, 256–265.
26. Fang, J.H., Zhang, Z.J., Shang, L.R., Luo, Y.W., Lin, Y.F., Yuan, Y., and Zhuang, S.M. (2018). Hepatoma cell-secreted exosomal microRNA-103 increases vascular permeability and promotes metastasis by targeting junction proteins. *Hepatology* *68*, 1459–1475.
27. Zhou, W., Fong, M.Y., Min, Y., Somlo, G., Liu, L., Palomares, M.R., Yu, Y., Chow, A., O'Connor, S.T., Chin, A.R., et al. (2014). Cancer-secreted miR-105 destroys vascular endothelial barriers to promote metastasis. *Cancer Cell* *25*, 501–515.
28. Park, H.J., Zhang, Y., Georgescu, S.P., Johnson, K.L., Kong, D., and Galper, J.B. (2006). Human umbilical vein endothelial cells and human dermal microvascular endothelial cells offer new insights into the relationship between lipid metabolism and angiogenesis. *Stem Cell Rev.* *2*, 93–102.
29. Valadi, H., Ekström, K., Bossios, A., Sjöstrand, M., Lee, J.J., and Lötvall, J.O. (2007). Exosome-mediated transfer of mRNAs and microRNAs is a novel mechanism of genetic exchange between cells. *Nat. Cell Biol.* *9*, 654–659.
30. Li, J., Liu, K., Liu, Y., Xu, Y., Zhang, F., Yang, H., Liu, J., Pan, T., Chen, J., Wu, M., et al. (2013). Exosomes mediate the cell-to-cell transmission of IFN- $\alpha$ -induced antiviral activity. *Nat. Immunol.* *14*, 793–803.
31. Leonardi, G.C., Candido, S., Cervello, M., Nicolosi, D., Raiti, F., Travalì, S., Spandidos, D.A., and Libra, M. (2012). The tumor microenvironment in hepatocellular carcinoma (review). *Int. J. Oncol.* *40*, 1733–1747.
32. Li, W., Zhang, L., Guo, B., Deng, J., Wu, S., Li, F., Wang, Y., Lu, J., and Zhou, Y. (2019). Exosomal FMR1-AS1 facilitates maintaining cancer stem-like cell dynamic equilibrium via TLR7/NF $\kappa$ B/c-Myc signaling in female esophageal carcinoma. *Mol. Cancer* *18*, 22.
33. Min, H., Sun, X., Yang, X., Zhu, H., Liu, J., Wang, Y., Chen, G., and Sun, X. (2018). Exosomes derived from irradiated esophageal carcinoma-infiltrating T cells promote metastasis by inducing the epithelial-mesenchymal transition in esophageal cancer cells. *Pathol. Oncol. Res.* *24*, 11–18.
34. Li, B., Song, T.N., Wang, F.R., Yin, C., Li, Z., Lin, J.P., Meng, Y.Q., Feng, H.M., and Jing, T. (2019). Tumor-derived exosomal HMGB1 promotes esophageal squamous cell carcinoma progression through inducing PD1<sup>+</sup> TAM expansion. *Oncogenesis* *8*, 17–34.
35. Wu, K., Huang, J., Xu, T., Ye, Z., Jin, F., Li, N., and Lv, B. (2019). MicroRNA-181b blocks gensenoside Rg3-mediated tumor suppression of gallbladder carcinoma by promoting autophagy flux via CREBRF/CREB3 pathway. *Am. J. Transl. Res.* *11*, 5776–5787.
36. Graham, A., Holbert, J., and Nothnick, W.B. (2017). miR-181b-5p modulates cell migratory proteins, tissue inhibitor of metalloproteinase 3, and annexin A2 during in vitro decidualization in a human endometrial stromal cell line. *Reprod. Sci.* *24*, 1264–1274.
37. Zhi, F., Shao, N., Wang, R., Deng, D., Xue, L., Wang, Q., Zhang, Y., Shi, Y., Xia, X., Wang, S., et al. (2015). Identification of 9 serum microRNAs as potential noninvasive biomarkers of human astrocytoma. *Neuro-oncol.* *17*, 383–391.
38. Zhi, F., Cao, X., Xie, X., Wang, B., Dong, W., Gu, W., Ling, Y., Wang, R., Yang, Y., and Liu, Y. (2013). Identification of circulating microRNAs as potential biomarkers for detecting acute myeloid leukemia. *PLoS ONE* *8*, e56718.
39. Zhi, F., Wang, Q., Deng, D., Shao, N., Wang, R., Xue, L., Wang, S., Xia, X., and Yang, Y. (2014). MiR-181b-5p downregulates NOVA1 to suppress proliferation, migration and invasion and promote apoptosis in astrocytoma. *PLoS ONE* *9*, e109124.
40. Chu, E.C., and Tarnawski, A.S. (2004). PTEN regulatory functions in tumor suppression and cell biology. *Med. Sci. Monit.* *10*, RA235–RA241.
41. Brognard, J., and Newton, A.C. (2008). PHLiPPing the switch on Akt and protein kinase C signaling. *Trends Endocrinol. Metab.* *19*, 223–230.
42. Harfouche, R., Hasséssian, H.M., Guo, Y., Faivre, V., Srikant, C.B., Yancopoulos, G.D., and Hussain, S.N. (2002). Mechanisms which mediate the antiapoptotic effects of angiotensin-1 on endothelial cells. *Microvasc. Res.* *64*, 135–147.
43. Maisonpierre, P.C., Suri, C., Jones, P.F., Bartunkova, S., Wiegand, S.J., Radziejewski, C., Compton, D., McClain, J., Aldrich, T.H., Papadopoulos, N., et al. (1997). Angiopoietin-2, a natural antagonist for Tie2 that disrupts in vivo angiogenesis. *Science* *277*, 55–60.
44. Tsigkos, S., Zhou, Z., Kotanidou, A., Fulton, D., Zakynthinos, S., Roussos, C., and Papapetropoulos, A. (2006). Regulation of Ang2 release by PTEN/PI3-kinase/Akt in lung microvascular endothelial cells. *J. Cell. Physiol.* *207*, 506–511.
45. Cheng, Y., Jiang, S., Hu, R., and Lv, L. (2013). Potential mechanism for endothelial progenitor cell therapy in acute myocardial infarction: Activation of VEGF- PI3K/Akte-NOS pathway. *Ann. Clin. Lab. Sci.* *43*, 395–401.
46. Ju, R., Zhuang, Z.W., Zhang, J., Lanahan, A.A., Kyriakides, T., Sessa, W.C., and Simons, M. (2014). Angiopoietin-2 secretion by endothelial cell exosomes: regulation by the phosphatidylinositol 3-kinase (PI3K)/Akt/endothelial nitric oxide synthase (eNOS) and syndecan-4/syntenin pathways. *J. Biol. Chem.* *289*, 510–519.